

---

## The Focal Surface of EUSO Telescope

---

H. M. Shimizu<sup>1</sup>, M. Ameri<sup>2</sup>, N. Bleurvacq<sup>3</sup>, F. Cadoux<sup>4</sup>, O. Catalano<sup>5</sup>, C. Chapron<sup>3</sup>, S. Cuneo<sup>2</sup>, T. Ebisuzaki<sup>1</sup>, F. Fontanelli<sup>6</sup>, V. Gracco<sup>6</sup>, P. Gorodetzky<sup>3</sup>, Y. Kawasaki<sup>1</sup>, Y. Miyazaki<sup>7</sup>, P. Musico<sup>2</sup>, M. Nagano<sup>7</sup>, P. Nedelec<sup>4</sup>, T. Patzak<sup>3</sup>, M. Pallavicini<sup>2</sup>, A. Petrolini<sup>2</sup>, E. Plagnol<sup>3</sup>, F. Pratolongo<sup>2</sup>, M. Sannino<sup>6</sup>, N. Sakaki<sup>1</sup>, Y. Takahashi<sup>8</sup>, M. Takeda<sup>1</sup>, Y. Takizawa<sup>1</sup>, M. Teshima<sup>9,\*</sup> and The EUSO Collaboration

(1) *RIKEN, 2-1 Hirosawa, Wako Saitama 351-0198, Japan*

(2) *INFN Genova, Via Dodecaneso 33, I-16146 Genova, Italy*

(3) *Physique Corpusculaire et Cosmologie, College de France, 11 place Marcelin Berthelot, F-75005 Paris, France*

(4) *Laboratoire d'Annecy-le-vieux de Physique des Particules, Chemin de Bellevue, BP 110, F-74941 Annecy-le vieux Cedex, France*

(5) *IASF-CNR Palermo, Via Ugo La Malfa 153, I-90146 Palermo, Italy*

(6) *Dipartimento di Fisica dell'Università di Genova, Via Dodecaneso 33, I-16146 Genova, Italy*

(7) *Fukui University of Technology, Gakuin, Fukui 910-8505, Japan*

(8) *Department of Physics, University of Alabama at Huntsville, Huntsville, Alabama 35899, U.S.A.*

(9) *Institute for Cosmic Ray Research, University of Tokyo, 5-1-5 Kashiwanoha, Kashiwa, Chiba 277-8582, Japan*

---

### 1. EUSO Telescope

The Extreme Universe Space Observatory (EUSO) is a space mission to study extremely high energy cosmic rays (EHECRs) in the energy region of  $10^{20}$  eV [1]. The EUSO instrument is a refractive telescope to be installed on the External Payload Facility of the Columbus module of the European Space Agency in the International Space Station, which views down the atmosphere of about 400 km diameter during its 3-year mission period. The EUSO telescope detects EHECRs by observing the time-resolved image of atmospheric fluorescence photons and Cherenkov photons accompanying the airshower. Atmospheric fluorescence photons are emitted mostly in near-ultraviolet wavelength region and dominant emission lines are located at the wavelengths of 337, 357 and 391 nm.

---

\* Present Address: Max Planck Institute für Physik, Föhringer Ring 6, 80805 München, Germany.

The EUSO optics consists of a pair of double-sided Fresnel lenses. Its field of view is  $60^\circ$  with  $f/\# = 1.25$  and the angular resolution of the optics is about  $0.1^\circ$ , which corresponds to about 4.5 mm r.m.s. spot size on the focal surface [2]. The observation with the large field of view optics from the altitude of about 400 km enables to enlarge the effective area, to measure the shower size as a function of time by correcting the relatively constant atmospheric attenuation and also to reconstruct the airshower in a well-defined geometry. The entrance pupil diameter is 2 m and the geometrical acceptance is about  $2 \times 10^{-11}$  sr at the center of the field of view.

## 2. Focal Surface Detector

The focal surface is an aspherical curved surface approximately parabolic of 2.3 m diameter, and its area amounts to about  $4.5 \text{ m}^2$ . The focal surface detector is designed as a closely packed mosaic of multianode photomultipliers (MAPMTs) approximating the curved focal surface, since it is required to detect the faint photon signals at the single photon sensitivity in the near-ultraviolet wavelength region of 330 – 400 nm on the basis of well-established detector elements[3,4]. Near-ultraviolet photons are selectively delivered on to the MAPMTs through optical filters. The focal surface should be segmented into pixels smaller than the spot size of the optics.

The strongest requirement for the focal surface detector is the maximization of the photon detection efficiency together with the uniformity over the focal surface. The overall efficiency of the focal surface detector ( $\epsilon_{\text{FS}}$ ) is given as the  $\epsilon_{\text{FS}} = \epsilon_1 \epsilon_2 \epsilon_3$ , where  $\epsilon_1$  is the geometrical occupancy of MAPMT units on the focal surface,  $\epsilon_2$  is the ratio of the sensitive area to the dimension of an MAPMT unit and  $\epsilon_3$  is the photon detection efficiency of MAPMT including the photocathode quantum efficiency and the photoelectron collection efficiency. The  $\epsilon_1$  depends on the arrangement of MAPMT array layout and  $\epsilon_1 \geq 0.9$  [5].

The MAPMT Hamamatsu R7600-M64 with UV-glass entrance window was assumed in the beginning of the conceptual design. The R7600-M64 has the anode format of  $8 \times 8$  in the central region of its entrance window and its  $\epsilon_2$  is 0.45. The value of  $\epsilon_2$  can be effectively improved by reducing the image on to the sensitive area employing additional components such as hemispherical refractive lens or tapered reflective pipe bundle on the top of MAPMT. The effective value of  $\epsilon_2 = 0.6\text{-}0.7$  is reasonably achievable.

For a larger  $\epsilon_2$ , we improved MAPMT having a grid electrode between the photocathode and the first dynode to weakly focus the photoelectrons on to the first dynode, which is referred to with the model number of R8900 (Hamamatsu) [6]. The sensitive area and anode segmentation projected back to the entrance window is shown in Fig. 2. for the case of  $6 \times 6$  anode format. Its has the value of  $\epsilon_2 = 0.83$  without additional component. The small dead area can be recovered

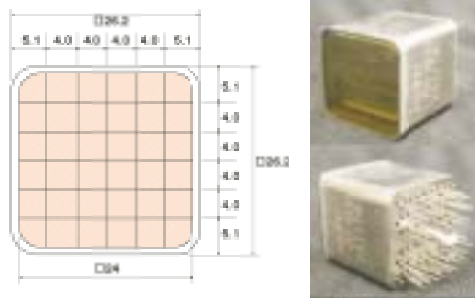


**Fig. 1.** The anode format projected on to the entrance window for the MAPMT Hamamatsu R8900-03-M36.

by inserting a tapered light guide to achieve  $\epsilon_2 > 0.9$  [4].

These MAPMTs have bialkali photocathode deposited on UV-glass and nominally  $\epsilon_3 = 0.15 \times (1 - 0.004(T/^\circ\text{C}))$  where  $T$  is the temperature.

As a result, the focal surface efficiency is  $\epsilon_{\text{FS}} = 0.12$  with R8900 MAPMT, which was  $\epsilon_{\text{FS}} = 0.08$  with R7600 MAPMT.

### 3. MAPMT R8900

The arrival direction of primary EHECRs will be measured by observing the axis of moving spots in the time-resolved images. The azimuthal angle can be determined from the direction of shower development, and the vertical angle can be determined from the difference of the apparent velocity of the moving spot and the speed of light. The Cherenkov photons reflecting on the earth surface or the top of the clouds gives additional information on the absolute altitude of the air shower. The accuracy of the determination of the arrival direction of EHECR and the atmospheric depth of the shower maximum is also adversely affected by enlarging the pixel size over the angular resolution of the telescope. The pixel size is limited also by the signal-to-noise ratio in a pixel since the contribution of the background photons is proportional to the area viewed by each pixel. The pixel size is selected so that it is comparable or smaller than the spot size of 4.5 mm, which corresponds to the anode segmentation of  $6 \times 6$  or finer assuming 1 mm spacing between R8900 MAPMT units.

The flight path of photoelectron is elongated compared with R7600 and receives more influence of external magnetic field. The influence of external magnetic field has been studied by observing the image distortion and by measuring the change of the gain of each anode under an external magnetic field. The magnetic field influence is largest when the field is normal to the entrance window, which corresponds to the vertical direction when the EUSO is installed. The decrease in the anode outputs was observed under the external magnetic field of 0.2 mT [6]. The vertical component of the geomagnetic field is expected to be varying

in the range of  $\pm 50\mu\text{T}$ , which is sufficiently small compared with the magnetic field influence.

The EUSO experiences the daytime and nighttime every 90 minutes. The temperature is designed to be monitored for the correction of the temperature dependence of  $\epsilon_3$ , which results in the  $\pm 5\%$  variation of  $\epsilon_3$  for the temperature change of  $\pm 10^\circ\text{C}$ . The heat flow must be considered carefully to stabilize the photodetector characteristics, in parallel with the heat dissipation of the electronics to be attached on the focal surface supporting structure.

#### 4. Summary

The overall detection efficiency of EUSO focal surface is  $\epsilon_{\text{FS}} = 0.12$  in the present design employing multianode photomultiplier with the weak electron focusing (R8900). It has been improved from the previous value of  $\epsilon_{\text{FS}} = 0.08$  designed with R7600 MAPMT.

Another possible focal surface detector is the array of R8400 series, which is often called as the flat-panel photomultiplier. The dimension of R8400 series is 52 mm  $\times$  52 mm. One unit of R9400 is compatible with four units of R8900 and the reconfiguration from R8900 to R8400 is straightforward. The value of  $\epsilon_2$  is 0.89 for R8400 without additional optical component on the top. The R8400-M256, which has the anode format of 16  $\times$  16, has been successfully developed [7]. We are ready to consider R8400-M256 as the candidate device as soon as the UV-glass version of R8400-M256 is successfully fabricated.

The value of  $\epsilon_3$  can be increased by improving MAPMT with higher quantum efficiency. A study to improve the quantum efficiency of single crystal photocathodes in near-UV wavelength region is in progress [8].

#### References

1. O. Catalano et al., in this conference.
2. R. Young et al., in this conference.
3. A. Petrolini et al., Nucl. Phys. B Proc. Suppl. **113** (2002) 329.
4. H. M. Shimizu et al., Proc. SPIE **4858** (2002) 219.
5. N. Bleurvacque et al., in this conference.
6. N. Sakaki et al., in this conference.
7. N. Inadama et al., IEEE Nuc. Sci. Sympo. & Med. Img. Conf. Record., M6-27 (2002).
8. M. Takeda et al., in this conference.